sustainability

MDPI

Article

Energy Evaluations of a New Plant Configuration for Solar-Assisted Heat Pumps in Cold Climates

Stefania Perrella *, Roberto Bruno, Piero Bevilacqua, Daniela Cirone and Natale Arcuri

Mechanical, Energy and Management Engineering Department, University of Calabria, V. P. Bucci 46/C, 87036 Rende, Italy
* Correspondence: stefania.perrella@unical.it

Abstract: Heat pumps in buildings allow for the limiting of CO_2 emissions by exploiting directly the renewable energy available in the external environment (aerothermal, hydrothermal and geothermal sources). Moreover, other renewable technologies such as active solar systems can be integrated easily into use with them. This combination not only increases the share of primary energy provided by renewable sources for heating/cooling but also improves the heat pump performance indices. Nevertheless, in cold climates, air–water heat pumps should be equally penalized due to the unfavorable outdoor air temperature. Conversely, a water–water heat pump, connected with a solar tank and thermal solar collectors, overcomes this issue. Indeed, the higher temperature attainable in the cold source allows for reaching greater COPs, and when the solar tank temperature level is enough, emitters can be directly supplied, avoiding the absorption of electric energy. In this paper, this plant configuration, in which a further tank after the heat pump was considered to manage the produced thermal energy, is investigated. Proper control strategies have been developed to increase the renewable share. Regarding a reference residential building located in Milan, for which the water–water heat pump was sized properly, a parametric study, carried out in TRNSYS by varying solar tank volume and collecting surface, has allowed for the identification of the optimal system configuration. A renewable share, ranging between 54% and 61% as a function of the collecting surface and the storage volume, was detected, as was an average seasonal coefficient of performance (SCOP) over 4. Regarding two common heating plant configurations using an assisted PV air-to-water heat pump and a gas boiler, the optimal solution allows for the limiting of CO_2 emissions by 33% and 53%, respectively.

Keywords: solar assisted heat pump; thermal storage; sustainable buildings; high-efficient energy buildings

Citation: Perrella, S.; Bruno, R.; Bevilacqua, P.; Cirone, D.; Arcuri, N. Energy Evaluations of a New Plant Configuration for Solar-Assisted Heat Pumps in Cold Climates. *Sustainability* **2023**, *15*, 1663. https://doi.org/10.3390/su15021663

Academic Editors: Concettina Marino and Antonino Nucara

Received: 28 November 2022
Revised: 10 January 2023
Accepted: 11 January 2023
Published: 14 January 2023

1. Introduction

The environmental challenge, aimed at combating dependence on fossil fuels, pollution and CO_2 emission, occupies a prominent place in the world panorama [1]. Conversely, the energy demand growth has to convey energy consumption towards a sustainable development model that promotes renewable energy sources [2]. In this context, the building sector plays a crucial role because it impacts considerably on the external environment, being responsible in the EU for 39.7% of the energy consumption of final uses and 36% of the greenhouse gas emissions [3]. In this field, a pragmatic solution that limits these percentages can be given by heat pumps [4]. Indeed, these devices can lead to exploiting renewable energy sources, including aerothermal, hydrothermal, geothermal and solar energy [5]. In the latter case, heat pumps are integrated with active solar systems to obtain the so-called "Solar-assisted Heat Pumps" (SAPH). In the literature, several studies are available concerning SAHP to use for heating, cooling and domestic hot water production. Yi Fan et al. have carried out a critical overview of research focused on SAHP. They have found that the principal weaknesses are: unsatisfactory energy performance at low temperatures, difficulty to couple solar collectors to reduce the absorption of electric energy and the lack of synchronism between thermal load demand and solar source availability for heating purposes [6]. Liang et al. studied the performance of a new air-source SAHP for building heating by TRNSYS simulations. The coefficient of performance (COP) of the air source heat pump increased with the solar collector area augment and, in the whole heating season, 40 m^2 of solar collector allowed to save 453.43 kWh [7]. L.Xu et al. have analyzed a system that combines an air-source heat pump connected to a storage tank. The water is also heated by a field of solar collector, to use both for DHW and space heating. The model was successively validated by experimental data. The authors found that the system performance is affected, respectively, by the outdoor air temperature, the tank volume and collector surface area [8]. The SAHP system can be integrated with thermal solar collectors, to use as the heat source, but also with photovoltaic (PV) panels to supply electricity as well as in hybrid configurations. For instance, Baker et al. have modelled a system in TRNSYS environment, composed of a ground source heat pump (GSHP) coupled with a field of 25 m^2 of photovoltaic-thermo (PV/T) panels, connected to a storage tank to use directly for space heating and DHW production, or send to the evaporator of the GSHP. They found that the system is able to cover the whole demand, both for heating and for the DHW [9].

According to the different integration modalities, SAHPs combined with thermal solar collectors are classified as direct (DX-SAHP) and indirect expansion solar-assisted heat pumps (IDX-SAHP). In the first case, thermal solar collectors and the heat pump evaporator are integrated into a single unit that uses solar energy to promote refrigerant evaporation. Charters et al. compared three technologies for producing DHW for the main Australian cities: a single solar thermal system, a single heat pump and a DX-SAHP. The comparison considered the electricity use, the life-cycle costs and the reductions in greenhouse gas emissions. The authors found that the right choice strongly depended on the climatic conditions and the local price of electricity [10]. Compared to the direct solar-assisted configurations, in indirect solar-assisted solutions (IDX-SAHP) thermal solar collectors and heat pumps were considered to be two independent systems. Banister et al. have developed an indirect dual-tank SAHP system for domestic hot water heating with a dedicated control strategy to minimize electricity consumption by selecting the best mode, experimentally validated, from those proposed. Annual simulations of system performance for a single-family residential home indicate that the dual-tank SAHP system provides significant energy savings in comparison to a traditional solar domestic hot water system [11]. Furthermore, IDX-SAHPs can be classified into three different functioning modes: series, parallel and dual-source systems. In the series and the dual-source modes, solar energy is employed to improve the heat pump performance, whereas in the parallel system the solar device and heat pump work together to increase the renewable share in energy demand. Usually, in a parallel system solar radiation is used to provide directly heating loads, however when solar radiation is not sufficient, the heat pump intervenes. Pinamonti et al. have analyzed the integration of a modulating water–water heat pump in a solar system equipped with a seasonal storage. System performance was evaluated through a series of energy simulations using TRNSYS [12].

The dual-source solar-assisted heat pump is designed to use two evaporators operating with different sources, choosing that with the most favourable temperature [13], but plant systems equipped with heat pumps operating with more than two sources have also been studied. In this regard, Emmi et al. have determined the performance of a multi-source energy system composed of PV/T solar collectors, heat pumps and two storage tanks, one for the heat source at the evaporator side, and the second one for the DHW production and the space heating of a single-family dwelling located in the Northeast of Italy. In particular, different sources (air, ground and water) were analyzed through the modelling of two plant configurations. The first does not contemplate the integration of solar radiation and thermal energy from the ground. In the second one, the system was conceived to use solar radiation to increase the ground thermal level. The simulations were carried out in a TRNSYS environment and showed that the latter solution was not economically profitable [14]. Liu et al. have proposed a dual-source heat pump (solar and air), used for space heating, in which the evaporator exchanges with the higher temperature between the air heated by the solar collectors and the external air. The performance of the dual-source heat pump has been studied and optimized, with various refrigerant and air flow rates supplying the solar collectors. The average monthly coefficient of performance of the dual-source heat pump can generally reach 3.6, and the average annual indoor temperature of the building is generally above 20 °C. One drawback of this installation setup is definitely the absence of a storage system that hinders a rational exploitation of solar surpluses [15].

In order to rationalize and increase the use of renewable sources and simultaneously improve the efficiency of the heat pump when operating in cold climates, this paper focuses on the possibility of combining a water–water heat pump with other renewable sources. The plant configuration involves a water–water heat pump, thermal solar collector, two thermal storage tanks and a PV generator with batteries. The tank connected with solar collectors is named the "solar tank", the second one is located after the heat pump and connected with the reference building ("secondary tank"). The basic purpose is to use solar thermal collectors and the solar tank to increase COPs by increasing the cold source temperature. When the temperature inside the solar tank is above 50 °C, the heating demand is met directly from the solar collectors through a motorized three-way valve that directly supplies the fan-coils of the reference building. The proposed system is able to overcome the limitation of air–water devices in cold climates due to the unfavorable outdoor air temperature that can hinder correct functioning. However, to avoid low COPs, the heat pump operation is allowed only when the solar tank temperature is over 5 °C. Alternatively, an auxiliary system (gas boiler), integrated into the secondary tank, intervenes. The system performances were investigated in a parametric study by varying solar tank volume and the collecting surface in simulations conducted in the TRNSYS environment. Proper control strategies were implemented in order to maximize the role of renewable sources to meet heating needs. System efficiency was assessed by considering:

- heating demand covered directly by the system, without considering the auxiliary intervention;
- system performance index regarding the non-renewable share;
- system performance index related to the renewable energy share;
- CO_2 emission level.

It is worth noting that the proposed plant, despite requiring a water thermal source, can be planned everywhere, and also for the renovation of existing heating systems. This paper, unlike other investigations already available in the literature, through parametric analysis, determines analytically the share of renewable energy and the correspondent level of CO_2 emissions that can be achieved, and the results were compared with two common solutions of heating plant: an air-to-water heat pump with a thermal storage system and which is connected to a PV generator, with qualities of a high energy performance and being easily installable, and the cheapest solution represented by a gas boiler.

2. Methods and Materials

In this section, the reference building plant system and numerical setup are presented. The main characteristic of the heat pump, the solar collector and the thermal storage are introduced. The description of the implemented control strategies is also described. Finally, how performance parameters are determined is outlined.

2.1. Case Study Building

The case study building (Figure 1) is the typical plan of a multi-storey building with a surface area of approximately 200 m^2 and an inter-floor height of 2.70 m. We decided to analyze a typical plan in order to generalize the application of the proposed system in other contexts. In fact, the surface investigated can be used for one, two or three flats, without losing its generality. In the present analysis, the standard plan consists of three flats surface (small, medium and large). The envelope was defined to satisfy current national regulations regarding the energy efficiency of buildings in Italy [16]. The main dispersing surfaces are represented by vertical walls, and the thermal properties of the layers are reported in Table 1. The building was simulated as a single thermal zone.

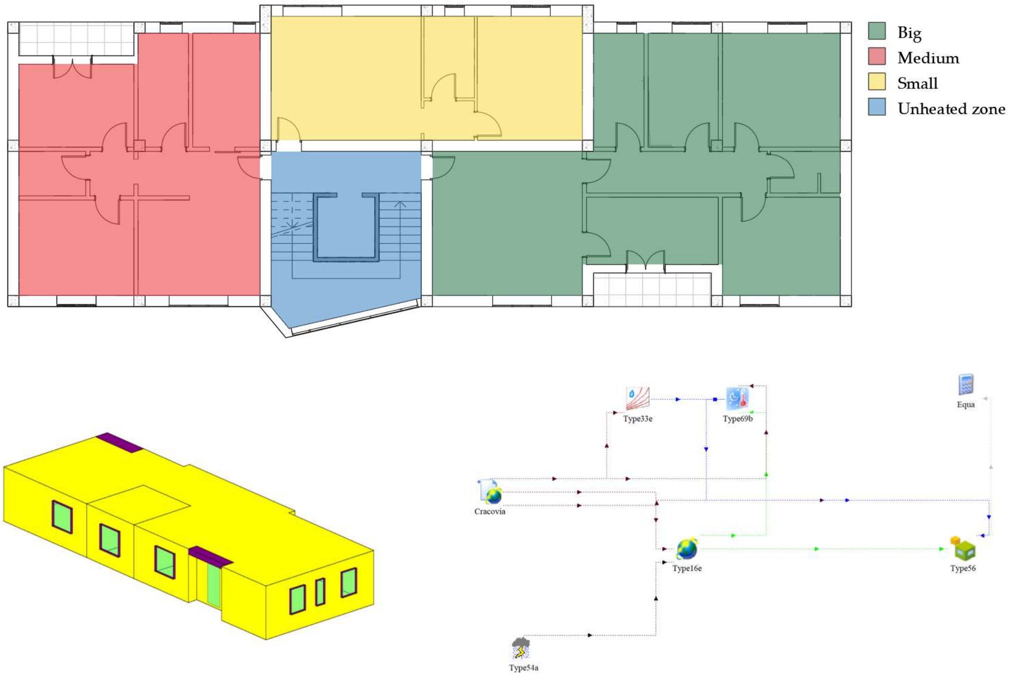

Figure 1. Case study building with flats locations and TRNSYS workspace for the design heating load evaluation.

Table 1. Thermal properties of the layers composing the external vertical wall.

		External Vertical Wall (U = 0.239 W/m^2 K)		
Material	**Thickness [cm]**	**Density [kg/m^3]**	**Specific Heat [J/kg K]**	**Thermal Conductivity [W/mK]**
Plaster	2	1400	1000	0.700
Bricks	30	850	1000	0.182 *
Insulation	8	70	1030	0.035
Skim Coat	2	1400	360	0.470
Plaster	1	1400	1000	0.700

* equivalent thermal conductivity.

For the aim of the study, the building is supposed to be located in Milan, characterized by a continental climate classified as subtype "CFb" (Marine West Coast Climate) in the Köppen Climate Classification [17]. This gives the location a dominant heating climate, whereas cooling requirements can be considered negligible. DHW needs, with a low magnitude in terms of energy requirements when compared with the heating ones, were neglected. Internal gains were defined according to the Italian National Standard UNI 11300-1, differentiating them according to a schedule [18]. Similarly, natural ventilation was assumed, with a rate of 0.3 air-change per hour (the minimum value imposed by the current Italian legislation for buildings intended as a Residence of a continuous character) [18]. Windows are made with a double-pane glazing 4/15/4, with an argon-filled wooden frame and a global thermal transmittance of 2.2 W/m^{2}K (frame-to-glazed surface ratio of 0.15). The heating loads required to size the heat pump have been quantified by using Type 56, with hourly weather data provided by CTI (Italian Thermo-technical Committee), as the typical meteorological year (TMY) [19]. It has to be noticed that transient simulations allow researchers to account for the capacity effects of the building fabric that affect the thermal balance of the building–plant system, and thus more reliable results were attained [20].

2.2. Heating Plant

The proposed system combines the use of solar thermal collectors, the solar tank at the service of the solar collector the secondary tank hosting the auxiliary system, a PV generator connected to batteries and a commercial water–water heat pump [21]. The building is conditioned by fan coils, supplied at 50 °C by the secondary tank.

2.2.1. Solar Thermal Collectors and Solar Tank

In order to limit winter thermal losses and exploit solar radiation more efficiently, evacuated heat pipe solar collectors have been used. The efficiency of the collector is defined by the following expression [17]:

$$\eta = \eta_0 - a_1 \cdot T_m - a_2 \cdot G \cdot T_m^2 \quad (1)$$

with optical efficiency (η_0) of 0.75, first order loss coefficient (a_1) of 1.18 $°C^{-1}$ and second order loss coefficient (a_2) equal to 0.0095 $m^2/W°C^2$ (the values are given in the correspondent datasheet of a commercial product. In the absence of data provided by the manufacturers, it is possible to use the parameters suggested by table C2 of the UNI 11300-4 standard) [22]. G is the incident solar radiation (W/m^2) and T_m the average water temperature (°C) inside the collectors, following the European approach. The solar collectors are tilted at 45°, while the surface area was varied from 8 to 40 m^2. The thermal energy supplying the heat pump evaporator is provided by a commercial solar tank, with a volume variable between 0.5 m^3 and 2 m^3, with constant height and changeable diameter, to limit temperature stratification effects in the vertical direction. The tank was simulated by a proper TRNSYS model without an internal coil on the heat pump side. Nevertheless, temperature stratification in the vertical direction was anyway considered. Technical features of the tanks are listed in Table 2.

Table 2. Main features of the simulated tanks.

	Solar Tank	**Secondary Tank**
Heat transfer fluid	Water	Water
Specific heat capacity	4.182 kJ/kg K	4.182 kJ/kg K
Fluid density	992 Kg/m^3	992 Kg/m^3
Thermal conductivity of the fluid	0.62 W/m K	0.62 W/m K
Max storage temperature	80 °C	80 °C
Tank volume	parametric	0.5 m^3
Tank height	1 m	1 m
Number of tank nodes	5	5
Top loss coefficient	0.923 W/m^2 K	0.923 W/m^2 K
Bottom loss coefficient	0.923 W/m^2 K	0.923 W/m^2 K
Edge loss coefficient	0.923 W/m^2 K	0.923 W/m^2 K

2.2.2. Water–Water Heat Pump

Preliminary simulations in design conditions allowed us to choose the appropriate heat pump rated power, an action performed by counting the highest percentage of hours during the heating period in which a precise power interval is required to assure an indoor set-point temperature of 20 °C. The results allowed for the identification of a commercial device with a rated heating capacity of 7.93 kW and a rated electric absorption of 2.10 kW (nominal coefficient of performance COP of 3.78). Figure 2 shows the trend of COP as a function of the temperature of the fluid at the evaporator for different values of water temperature at the condenser.

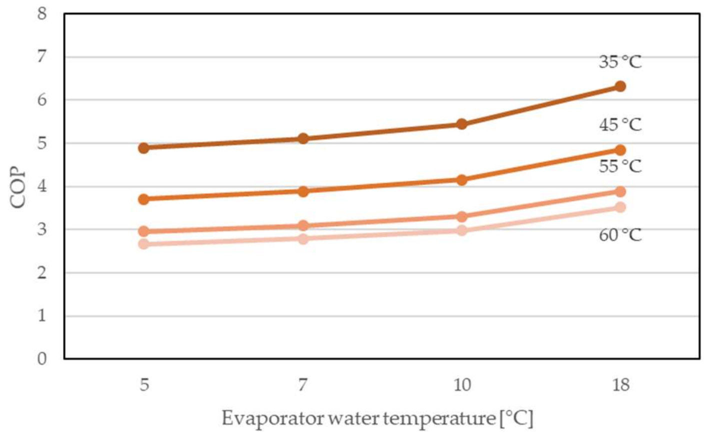

Figure 2. Trend of the heat pump COP as a function of the condenser temperature.

Table 2 listed main features of the simulated tanks (the values are given in the correspondent datasheet) while in Table 3, instead, the main features of the heat pump are reported [17]. The device is equipped with an inverter and the accurate sizing allows us to avoid further COP worsening due to the operation in part-load mode. The heat pump condenser supplies the secondary tank, whose features are similar to those of the solar tank (see Table 2), except for the storage volume that was set constant to 0.5 m^3.

Table 3. Main properties of the water–water heat pump.

Heat Pump	
Type	Water-to-Water
Rated Heating Capacity	7.93 kW
Rated COP	3.78
Evaporator water flow rate	1722 l/h
Condenser water flow rate	1369 l/h

2.2.3. PV Generator and Electrical Storage

To improve the energy share derived from renewable sources, 6 kW_p (36 m^2) of PV poly-crystalline panels (with properties listed in Table 4 [23]) and grid-connected were considered for the provision of a part of the required electric energy [24,25].

Table 4. Electrical Characteristics of PV Panels.

Photovoltaic Panels Feature	
Panel type	Polycrystalline silicon
Area	1.627 m^2
Nominal Power	280 W
Panels number	22
Voltage at max power	31 V
Current at max power	9.07 A
Short-circuit current	9.76 A
Open circuit voltage	38 V
Temperature coefficient of I_{sc}	−0.31%/°C
Temperature coefficient of V_{oc}	0.05%/°C
NOCT	45 °C
Nominal efficiency	0.15

The size of the PV generator was chosen based on the available roof surface, moreover 6 kW represents the threshold values that allow for the installation of a mono-phase electric plant, as stated by the current Italian regulation. Being the non-synchronism between required electric loads and the availability of solar radiation, the same generator was equipped with an electric storage system to better manage the PV power output surpluses. The simulated batteries were assumed to have a capacity of 6000 Wh.

2.3. Implemented Control Strategies

A scheme of the proposed plant, simulated in the TRNSYS environment, is depicted in Figure 3. Figure 4, instead, shows a flow chart describing the control strategies conceived to increase the renewable share in heating requirements. It can be noticed that the pump of the solar circuit is activated when the outlet temperature from solar collectors is 5 °C higher than the temperature detected at the bottom of the solar tank. Furthermore, the same pump is turned off when the temperature inside the solar tank exceeds 80 °C on the top side. When the temperature level inside the solar tank is above 50 °C, the hot water is directly used to supply fan-coils by acting on a three-way valve that bypasses the heat pump, which conversely is activated when the storage temperature ranges between 5 °C and 50 °C. When the continuous hot water withdrawal from the solar tank causes an abrupt temperature drop, the control system inactivates the heat pump to avoid freezing phenomena, and simultaneously an auxiliary system, represented by a gas boiler connected to the secondary tank, is activated. When the tank connected with the heat pump condenser exceeds 50 °C (the heat pump can operate also at 60 °C), another motorized valve regulates water temperature, supplying fan-coils to 50 °C by recirculating a fraction of the returned flow rate.

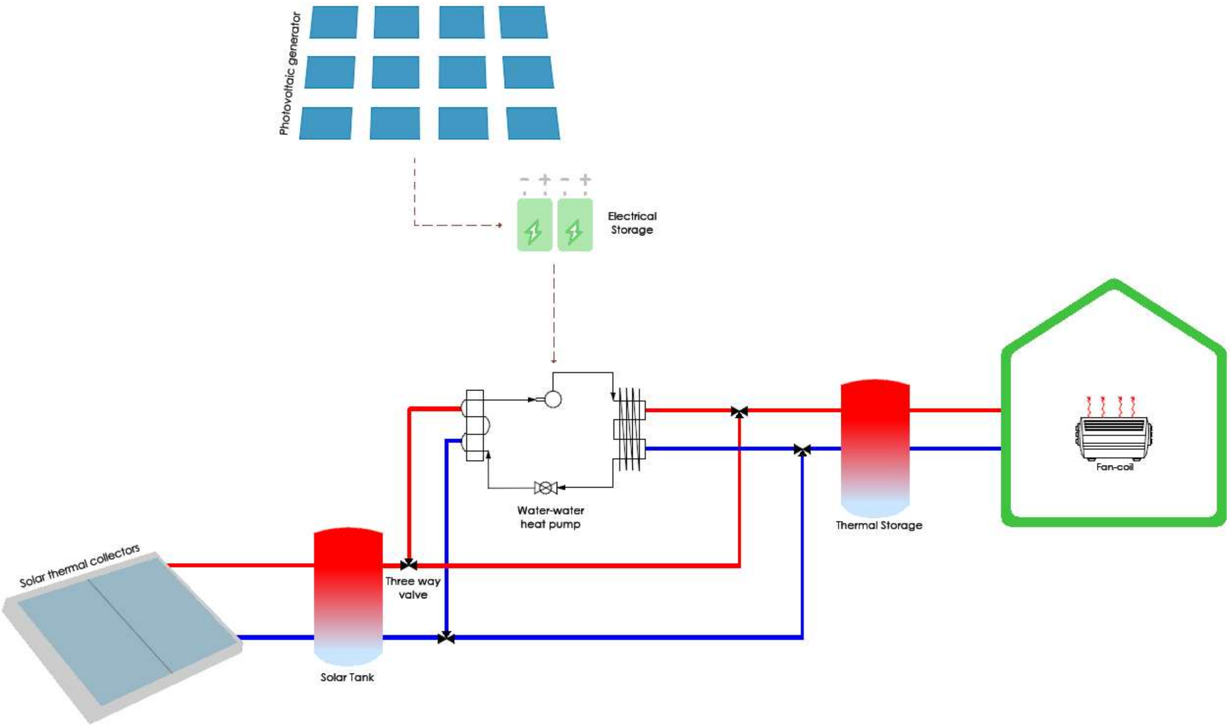

Figure 3. Scheme of the simulated SAHP.

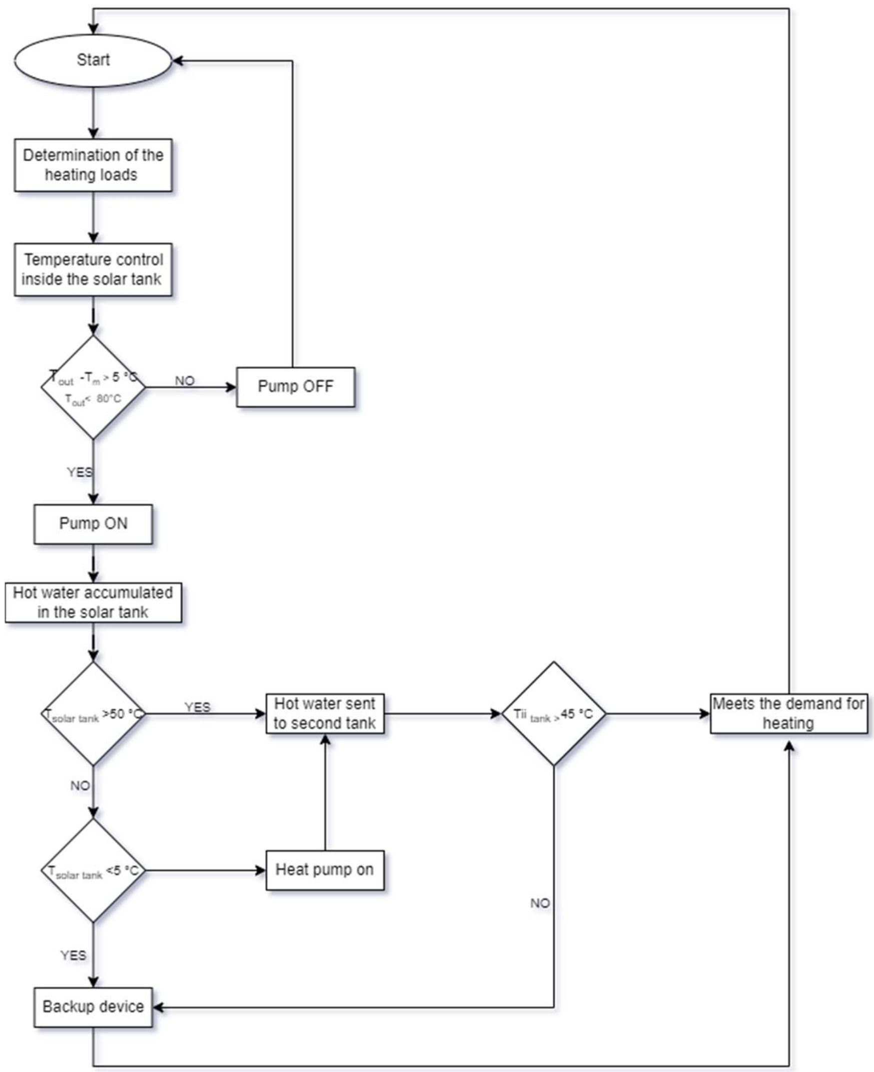

Figure 4. Flow chart describing the control strategies adopted for the heating plant.

2.4. Simulation Model

The simulation model was developed in a TRNSYS 18 environment [26]. It has to be noticed that the heat pump model was validated by comparison with experimental data of a similar heating plant located at the University of Calabria under typical Mediterranean climatic conditions [27]. To determine the thermal performances in Milan, the building–plant system was simulated by TRNSYS with actual weather data. In light of this, it is worth noting that the obtained performances are relevant to the statistical data reported in the European project TABULA for a similar building typology (multi-storey building) built after 2005 [28]. Simulations were also carried out to determine the performances of other plant configurations, employing a PV assisted air–water heat pump without batteries, albeit with a thermal storage system (easy to install and with a high share of renewable primary demand), and the cheapest solution of a gas boiler supplying radiators.

2.5. Primary Energy Consumption and Emission Levels

The concept of primary energy factor (PEF) has been chosen by European Community to determine and compare the primary energy demand of different plant configurations in which diverse energy carriers are involved. In particular, PEF allows for the calculation of the total primary energy needed to produce a unit of particular final energy consumed. It includes energy extraction, transmission, storage, distribution and the losses related to the processes. Accordingly, the PEFs reflect the reality of a complete energy system, from energy production to final consumption [29]. In Table 5, some values related to the energy carriers involved in the proposed system, which follows the current Italian regulation, are reported.

Table 5. PEFs and CO_2 emission factors defined according to the Italian national standard.

Energy Carrier	$PEF_{,nren}$	$PEF_{,ren}$	$PEF_{,tot}$	$kgCO_{2eq}/kWh$
Natural gas	1.05	0	1.05	0.21
Electricity energy from the grid	1.95	0.47	2.42	0.46
Electricity from PV	0.00	1.00	1.00	0.00
Thermal solar collector	0.00	1.00	1.00	0.00

3. Results

The system performances are assessed through the following parameters:

- the heating demand covered directly by the system without the intervention of the auxiliary generator, as a function of the collecting surface and solar tank volume;
- the seasonal non-renewable performance index, defined as the ratio between the primary energy supplied to the building and the energy absorbed from the external environment;
- the share of the renewable energy employed for covering the heating demand;
- the CO_2 emission level.

3.1. Calculation of the Heating Needs of the Reference Building in the Considered Climate

Figure 5 shows the heating energy requirement (red line) amounts to 12,614 kWh considering the actual weather data associated with the TMY available for Milan. It can be noticed that the maximum hourly energy for heating is slightly over 6 kWh, which differs from the value determined in design conditions because the latter is determined with a constant set-point outdoor air temperature (−5 °C). Furthermore, it can be appreciated that the heating period starts in October and finishes in April, confirming the dominant heating climate. Despite cooling loads also reaching 3 kW, these could be further limited by considering in the simulations the adoption of passive solutions such as shading systems on the transparent surfaces and nightly free-cooling, making them negligible when compared to the heating needs. In order to justify the choice of heat pipe technology, Figure 6 reported the total horizontal radiation for Milan between October and April, highlighting the scarce availability of solar radiation that is accompanied by the low values of outdoor air temperature.

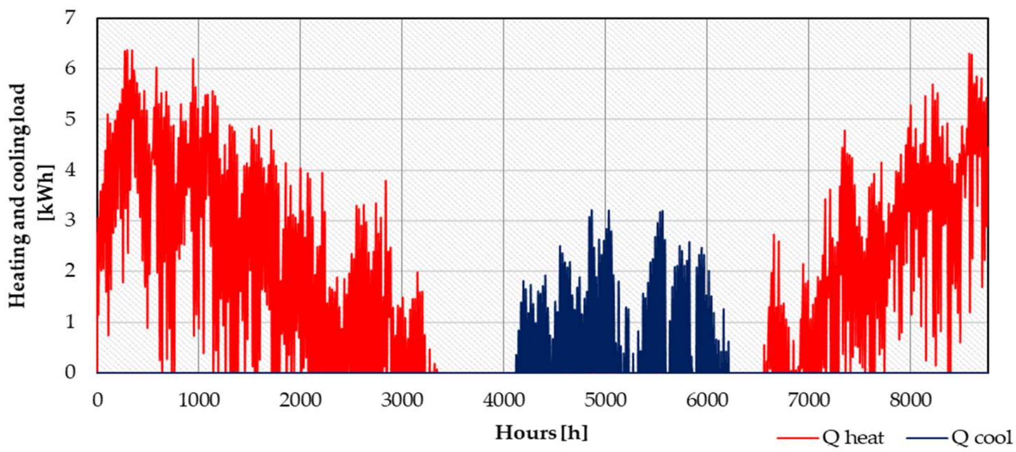

Figure 5. Heating and cooling load for the locality of Milan using TMY for weather data.

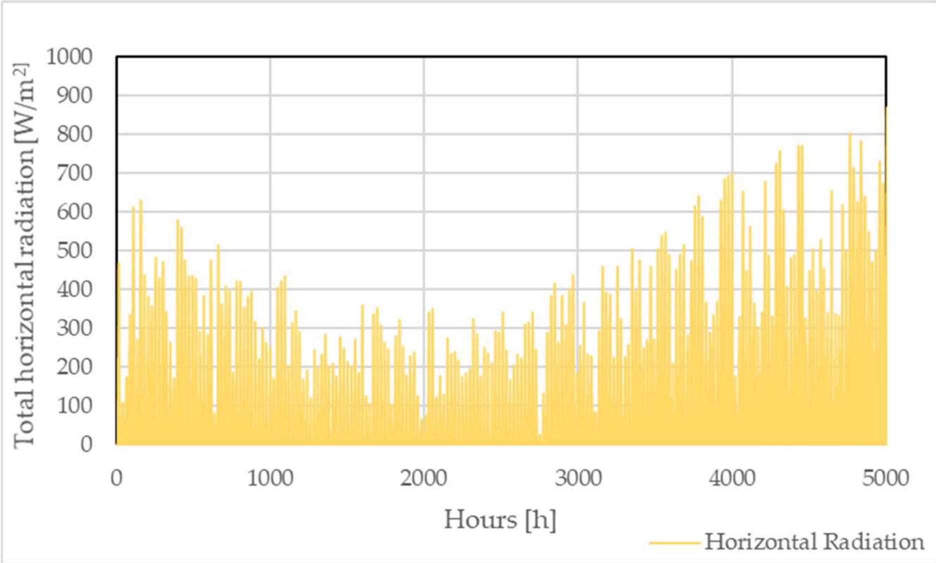

Figure 6. Total Horizontal Radiation for Milan between October and April.

3.2. System Operational Description

Figure 7 shows the percentage of demand covered by each source involved in the proposed heating plant as a function of the collecting surface and the solar tank volume. In particular, the light green dashed bar represents the share covered directly by solar collectors without the heat pump intervention (by the three-way motorized valve), the red bar is the share covered by the auxiliary system (gas boiler) and finally in the dark green dashed line shows the share provided by the water–water heat pump. It is worth noting that the solar field is mainly involved with large thermal collector surfaces and limited storage tank volumes. Conversely, the heat pump is used more frequently, with a large collector surface and high solar tank volumes. The functioning of the auxiliary system is reduced under 50% of the heating hours only when the thermal collector surface is greater than 24 m^2, however the percentage reduces with the collection surface and the solar tank volume growth. This means that the beneficial effect of the solar tank volume growth on the heat pump functioning prevails on the limitation of the share directly provided by the solar field.

Globally, the percentage of the demand covered by the proposed system increases with the solar tank volume, but it nevertheless weighs less than the collection surface. The percentage covered by the heat pump and thermal solar collectors is about 20–21%, with a collecting surface of 8 m^2 for every solar tank volume, and this share increases up to 62% for a volume of 2 m^3 and 40 m^2 of collecting surface. The share of energy needs covered directly by the system increases considerably from 8 m^2 to 16 m^2 and from 16 m^2 to 24 m^2, while it is negligible for further increases of the collecting surface.

Figure 7. Percentage of the heating demand covered by the different generators as a function of collecting surface S (m^2) and solar tank volume V (m^3).

3.3. Electric Energy Demand and CO_2 Emission

Starting from the demand supply by each source, the consumptions of heat pump and auxiliary system are determined. In Table 6, for each combination, the electrical consumption of the heat pump and the gas consumption of the boiler on a seasonal basis is reported as a function of collecting surface S (m^2) and solar tank volume V (m^3).

Table 6. Winter electric and gas consumption in the analyzed heating plant.

S (m^2)	V = 0.5 m^3		V = 1 m^3		V = 1.5 m^3		V = 2 m^3	
	kWh_{ele}	kWh_{gas}	kWh_{ele}	kWh_{gas}	kWh_{ele}	kWh_{gas}	kWh_{ele}	kWh_{gas}
8	695	11,765	746	11,616	771	11,538	785	11,483
16	846	9676	969	9333	1033	9156	1069	9048
24	919	8443	1074	7951	1158	7695	1216	7550
32	956	7636	1148	6996	1252	6660	1304	6467
40	983	7084	1172	6331	1294	5938	1369	5705

A considerable portion of the electricity consumption (green bar of Figure 8) due to the use of the heat pump is supplied by the PV system combined with the batteries (in red the share covered by the grid, in grey the m^3 of gas consumed by the auxiliary boiler). With the augment both in solar collector surface and the volume of the solar tank increases the percentage of heating demand supply directly by the solar-assisted heat pump. For this reason, the electricity consumption increases but simultaneously the consumption of gas decreases drastically. It is worth noting that, from a PV utilization viewpoint, a collecting surface of 16 m^2 is preferable because a sort of ideal combination between PV production and heat pump operation was found. For the other cases, the share covered by the PV generator is almost constant, and rather tends to slightly decrease with the collection surface growth. Similarly, the storage tank volume does not affect the PV share considerably, whereas the augmentation of the collection surface produces an evident increase in the electricity withdrawal from the grid due to the wider operation time of the heat pump.

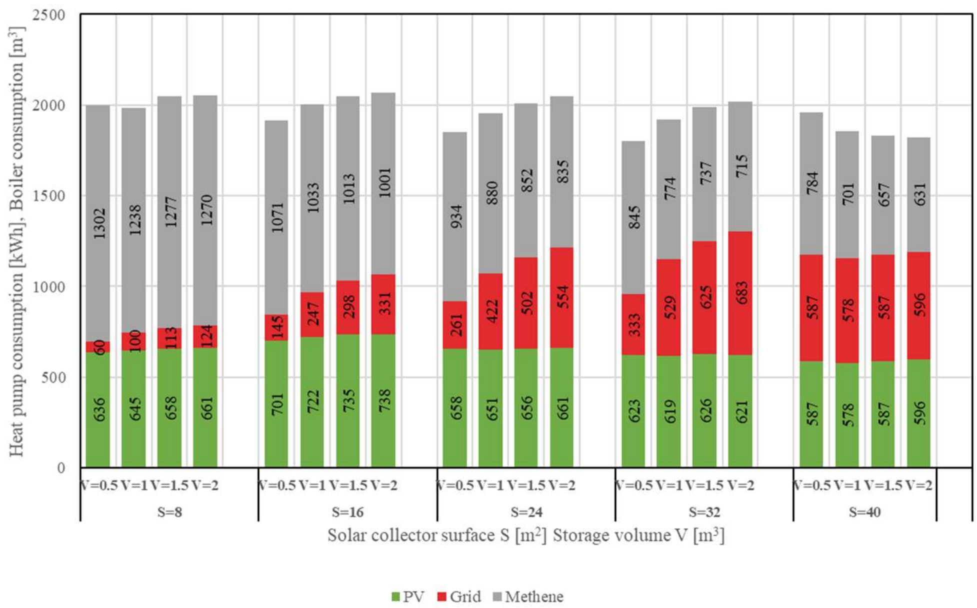

Figure 8. Consumptions of gas and electricity in the proposed system as a function of collecting surface S (m^2) and solar tank volume V (m^3).

Considering the primary energy factors reported in Table 5, starting from the calculated consumption reported in Table 6, the renewable and non-renewable primary energy associated with each analyzed configuration were listed in Table 7.

Table 7. Renewable and non-renewable primary energy shares as a function of collecting surface (S) and solar tank volume (V).

S (m^2)	V = 0.5 m^3		V = 1 m^3		V = 1.5 m^3		V = 2 m^3	
	Ep_{ren} [kWh]	Ep_{nren} [kWh]	Ep_{ren} [kWh]	Ep_{nren} [kWh]	Ep_{ren} [kWh]	Ep_{nren} [kWh]	Ep_{ren} [kWh]	Ep_{nren} [kWh]
8	664	12,470	692	11,941	771	12,336	720	12,292
16	769	10,445	839	10,282	875	10,192	893	10,143
24	780	9371	850	9173	891	9063	921	9003
32	780	8867	867	8377	919	8211	942	8116
40	863	8210	850	7811	863	8116	877	7149

Moving from 8 m^2 to 40 m^2 of collecting surface, independently from the storage volume, a reduction in non-renewable primary energy by about 30% was attained. Furthermore, the renewable share slightly varies with the solar thermal collector area, whereas noticeable deviances have been reordered by increasing the volume of the solar tank.

The system performance index (Figure 9) was calculated as the ratio between the thermal energy demand and the non-renewable share of primary energy, and so high values denote a plant configuration with an elevated share of renewable energy to satisfy heating needs. This index shows that system performance, in general, improves with the solar collector area growth, passing from 0.95 with 8 m^2 and 0.5 m^3, up to 1.592 with 40 m^2 and 2 m^3. However, the differences detected by varying the storage volume are negligible. Basically, the percentage of needs covered by the system increases in an evident manner moving, from 8 to 40 m^2 of the collecting area rather than the increase in the volume of the solar tank. Figure 8 shows the trend of the seasonal COP, which slightly varies around 4.29–4.32 for every heating plant configuration, demonstrating that the solar-assisted heat pump is able to operate with a high-performance index in the considered climatic condition, when compared with the rated values. The COP enhanced by 1.4% only, but this increase determines that a high share of the primary renewable share is employed by the proposed system. In particular, these values are greater than those provided by the manufacturer every time the supply hot water is over 45 °C and the inlet temperature at the evaporator is lower than 10 °C.

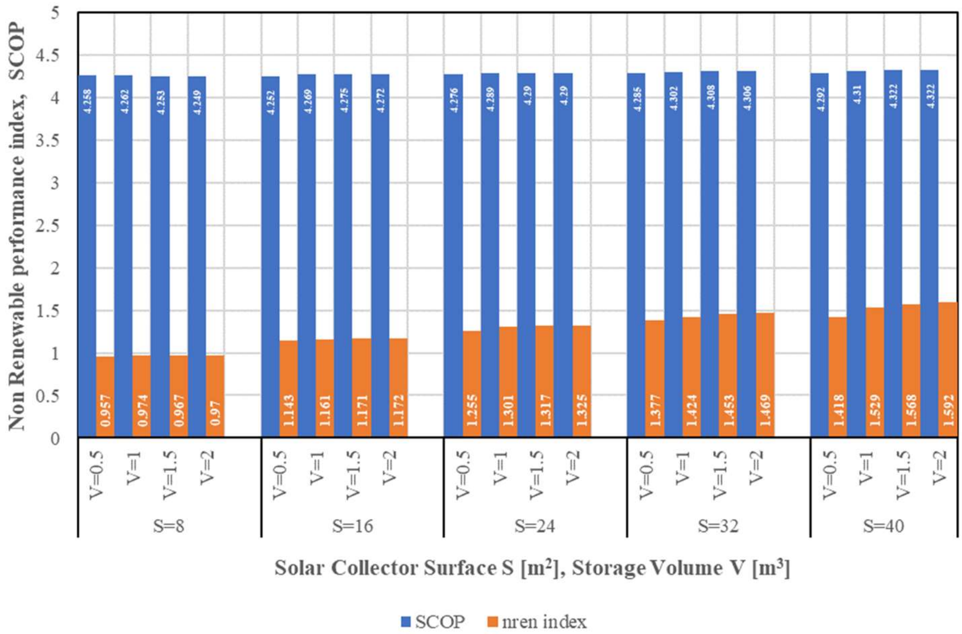

Figure 9. Trend of non-renewable performance index as a function of collecting surface S (m^2) and solar tank volume V (m^3).

When the proposed system is compared with the alternative heating plant using an assisted PV air-to-water heat pump and a storage tank (system 1), primary energy consumption of 5349 kWh was recorded. Only 990.25 kWh are supplied by the PV system, while the remaining is absorbed from the grid. The share of non-renewable primary energy is determined for both systems and these values are reported in Figure 10. It is possible to appreciate that, for solar collector surfaces larger than 24 m^2, the proposed system is more performant than the air–water heat pump in light of the lower shares of non-renewable primary energy. The percentage reduction varies between 4% and 8%, with 24 m^2 of solar collectors for the different solar tank volumes. The reduction is bigger in the correspondence of 32 m^2 of the collecting area being 17%. The greatest decrease is recorded for a surface of 40 m^2 and a storage volume of 2 m^3.

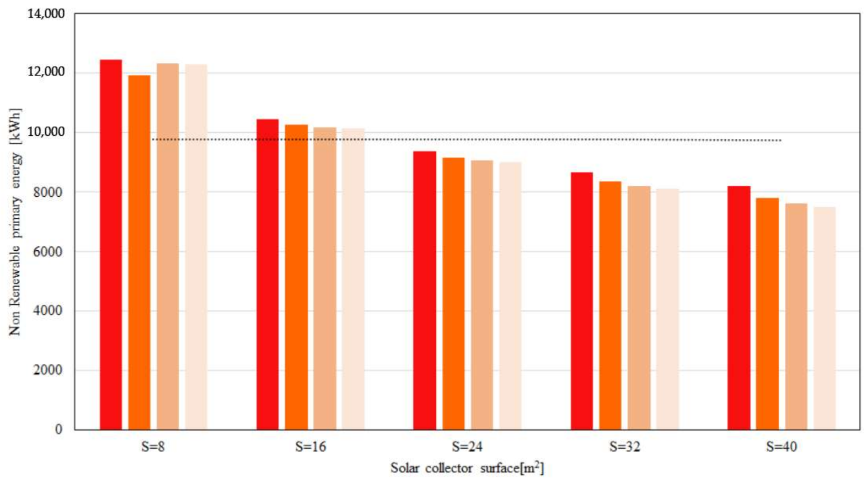

Figure 10. Comparison between the non renewable Energy primary index as a function of collecting surface, S (m^2), and solar tank volume, V (m^3). The color gradient from dark to light represents V = 0.5, V = 1, V = 1.5, V = 2.

When the proposed system, instead, is compared to a traditional gas boiler (system 2, for which an average seasonal efficiency of 0.8 was assumed) a consumption of 14,915 kWh was determined, with a share of non-renewable primary energy of 15,661 kWh (Table 8). Regarding the previous heating plant configurations, the gas boiler obviously determines the highest consumption and the highest share of non-renewable primary energy. Table 9 details the percentage variation in non-renewable primary energy of each combination, compared to system 1 and system 2.

Table 8. Non-renewable primary energy (Ep_{nren}) for all heating plants analysed.

S (m²)	**Ep_{nren} [kWh]**			
	V = 0.5 m³	**V = 1 m³**	**V = 1.5 m³**	**V = 2 m³**
8	12,470	11,941	12,336	12,292
16	10,445	10,282	10,192	10,143
24	9371	9173	9173	9003
32	8867	8377	8377	8116
40	8210	7811	7811	7496
Air-to-Water Heat Pump	9791.7			
Boiler	15,661			

Table 9. Percentage reduction of non-renewable primary energy of each combination compared to system 1 and system 2.

	V = 0.5 m³		**V = 1 m³**		**V = 1.5 m³**		**V = 2 m³**	
S (m²)	**System 1**	**System 2**	**System 1**	**System 2**	**System 1**	**System 2**	**System 1**	**System 2**
8	27.35%	−20.38%	21.95%	−23.75%	25.98%	−21.23%	25.53%	−21.51%
16	6.67%	−33.31%	5.01%	−34.35%	4.09%	−34.92%	3.59%	−35.23%
24	−4.30%	−40.16%	−6.32%	−41.43%	−7.45%	−42.14%	−8.05%	−42.51%
32	−9.44%	−43.38%	−14.45%	−46.51%	−16.14%	−47.57%	−17.11%	−48.18%
40	−12.34%	−45.20%	−20.57%	−50.34%	−24.65%	−52.89%	−26.99%	−54.35%

Figure 11 shows the comparison of the share of renewable and non-renewable energy for the three considered configurations of the heating plant.

As a consequence of the lowest non-renewable primary energy demands, the proposed system also allows for a noticeable reduction in CO_2 emissions (Figure 12). The equivalent emissions have been calculated through the factors listed in Table 5 as a function of the energy carrier. It is possible to appreciate how, compared with a traditional system in which the total thermal load is provided only by a gas boiler, the equivalent CO_2 emissions are lower for each plant configuration. When the system, instead, is compared with the assisted PV air-to-water heat pump, the equivalent CO_2 emissions are always lower, except for a collecting surface of 8 m^2. Globally, the equivalent CO_2 emissions decrease with the solar collector area growth and less with the increase in the accumulation volume. In its best configuration, the proposed system produces a reduction by 33% of emitted CO_2 if compared with the air–water heat pump, and 53% if compared with the gas boiler.

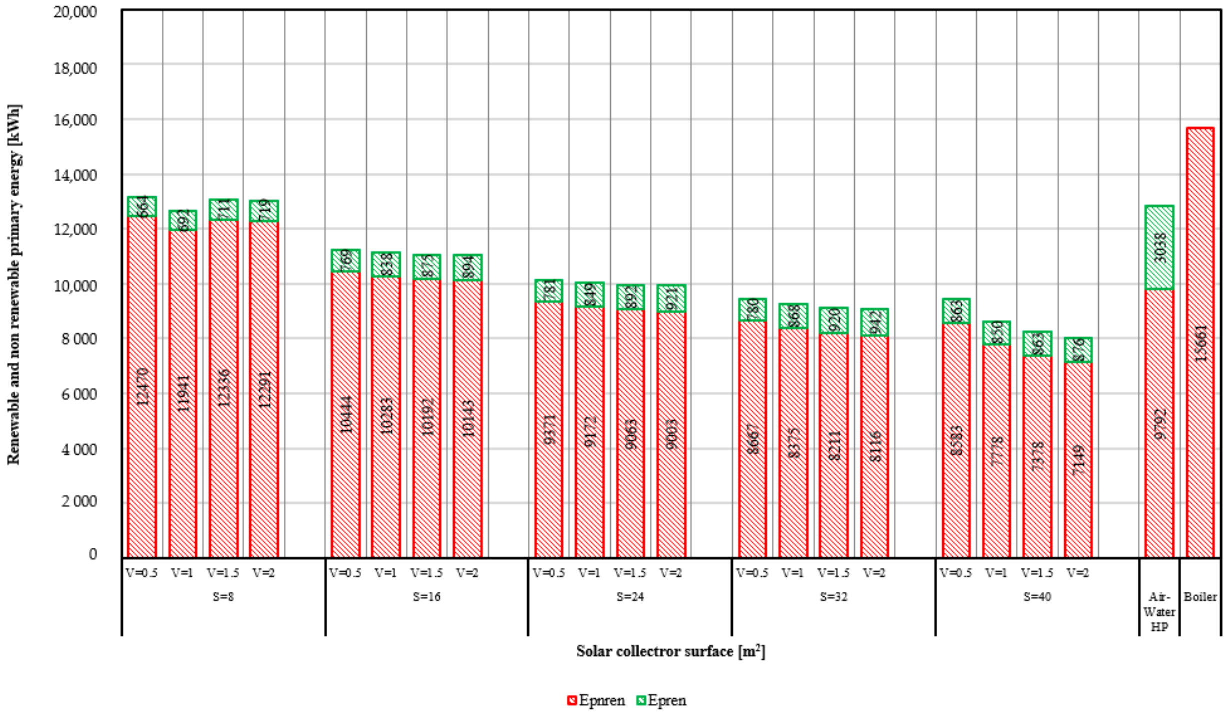

Figure 11. The share of total primary energy, including renewable and non-renewable energy for all the systems compared.

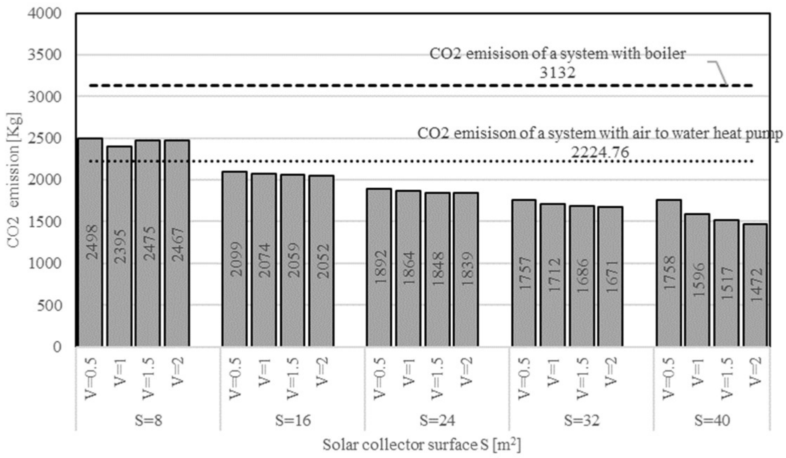

Figure 12. Comparison of the CO_2 emissions between the proposed SAHP and the heating plants equipped with assisted PV air–water heat pumps and equipped with a gas boiler.

4. Conclusions

This study deals with the energy and environmental evaluations concerning a SAHP system conceived for cold climates that combines the use of solar collector panels, a water–water heat pump, two storage tanks and a photovoltaic system with batteries. Such a combination and the development of proper control strategies allow for the better exploitation of the active solar systems, also using solar radiation to directly operate the space heating or, alternatively, to improve the heat pump performance. The electric consumptions are reduced by means of the better COPs. Furthermore, the batteries allow to overcome efficiently the mismatching between solar radiation availability and thermal load request. The system performances were investigated by a parametric study by varying solar tank volume and the collecting surface. From the results analysis, it emerged that the system ensures excellent heat pump performance, with an average COP always greater than 4, with the rated value of the simulated commercially available device being 3.78. The heating demand covered by the proposed system increases both with the collecting surface area and the solar tank volume growth, and a percentage of 22% can be provided directly by 40 m^2 of solar collectors with a solar tank volume of 0.5 m^3.

The percentage covered by the combined use of heat pump and thermal solar collectors moves from 20–21% with a collecting surface of 8 m^2, up to 62% for a volume of 2 m^3 and 40 m^2. Regarding the primary energy demand, the same configuration permits attaining the lowest non-renewable share. If compared with a heating plant using an assisted PV air-to-water heat pump and a thermal storage system, a decrease by 27% of the required primary energy was detected, because this system in continental climates suffers from unfavorable outdoor air temperatures. The percentage increases up to 54% when the proposed system is compared with the widespread heating plant solution equipped with a gas boiler, corresponding to a CO_2 emissions reduction by 53%.

Currently, the cheapest solution for building builders is represented by a heating plant using a gas boiler supplying radiator. Nevertheless, this solution leads to an energy performance index of about 78 kWh/m^2 per year. The proposed system allows for a drastic reduction of the energy consumption, producing energy performance indices ranging between 37 kWh/m^2 and 62 kWh/m^2, the latter detected with 8 m^2 of collecting surface and 0.5 m^3 of storage volume. These values confirm that the wider investment costs required for the installation of the proposed SAHP are properly counterbalanced by appreciable economic savings achievable by the limitation of operative expense.

In successive investigations, the same plant, equipped with a cooling tower and/or air cooler, will be investigated in the summer period to determine energy performance at an annual level, which is performed to carry out an economic analysis aimed at evaluating the profitability of the investment. Furthermore, the same plant, equipped with a radiant emission system, will be investigated in order to compare the performance of the system and the comfort indoor.

Author Contributions: Conceptualization, S.P. and R.B.; Data curation, S.P.; Methodology, S.P.; Resources, S.P.; Visualization, D.C.; Writing—original draft, S.P. and D.C.; Writing—review & editing, R.B., P.B. and N.A. All authors have read and agreed to the published version of the manuscript.

Funding: The research was partly supported by the Italian National Operational Programme (PON) Research and Innovation" 2014/2020—Axis II—specific target 1.b) with the research project ARS01_00836 "COGITO—A COGnItive dynamic sysTem to allOw buildings to learn and adapt.

Conflicts of Interest: The authors declare no conflict of interest.

References

1. IEA. Data and Statistics. Available online: https://www.iea.org/data-and-statistics (accessed on 15 June 2021).
2. Bruno, R.; Arcuri, N.; Carpino, C. The passive house in Mediterranean area: Parametric analysis and dynamic simulation of the thermal behavior of an innovative prototype. *Energy Procedia* **2015**, *82*, 533–539. [CrossRef]
3. IEA. *Tracking Buildings 2020*; IEA: Paris, France, 2020.
4. Arcuri, N.; Bruno, R.; Carpino, C. PV driven heat pumps for the electric demand-side management: Experimental results of a demonstrative plant. In Proceedings of the 2018 IEEE International Conference on Environment and Electrical Engineering and 2018 IEEE Industrial and Commercial Power Systems Europe (EEEIC/I&CPS Europe), Palermo, Italy, 12–15 June 2018; IEEE: Piscataway, NJ, USA, 2018; pp. 1–6. [CrossRef]
5. Arcuri, N.; Bruno, R.; Bevilacqua, P.; Carpino, C. Strategies for the reduction of electricity consumptions in heat pumps: The role of the thermal inertia in buildings equipped with radiant systems. In Proceedings of the BS2019, Rome, Italy, 2–4 September 2019; pp. 1724–1731. [CrossRef]
6. Fan, Y.; Zhao, X.; Han, Z.; Li, J.; Badiei, A.; Golizadeh, Y.; Liu, Z. Scientific and technological progress and future perspectives of the solar assisted heat pump (SAHP) system. *Energy* **2023**, *229*, 120719. [CrossRef]
7. Liang, C.; Zhang, X.; Li, X.; Zhu, X. Study on the performance of a solar assisted air source heat pump system for building heating. *Energy Build.* **2011**, *43*, 2188–2196. [CrossRef]
8. Xu, L.; Zhang, Y.; Luo, X. Applicability and comparison of solar-air source heat pump systems between cold and warm regions of plateau by transient simulation and experiment. *Build. Simul.* **2021**, *14*, 1697–1708. [CrossRef]
9. Bakker, M.; Zondag, H.A.; Elswijk, M.J.; Strootman, K.J.; Jong, M.J.M. Performance and costs of a roof-sized PV/thermal array combined with a ground coupled heat pump. *Sol. Energy* **2005**, *78*, 331–339. [CrossRef]
10. Charters, W.W.S.; Chaichana, C. Solar heat pump systems for domestic hot water. *Sol. Energy* **2002**, *73*, 169–175.

11. Banister, C.J.; Collins, M.R. Development and performance of a dual tank solar-assisted heat pump system. *Appl. Energy* **2015**, *149*, 125–132. [CrossRef]
12. Pinamonti, M.; Beausoleil-Morrison, I.; Prada, A.; Baggio, P. Water-to-water heat pump integration in a solar seasonal storage system for space heating and domestic hot water production of a single-family house in a cold climate. *Sol. Energy* **2021**, *213*, 300–311. [CrossRef]
13. Buker, M.S.; Riffat, S.B. Solar assisted heat pump systems for low temperature water heating applications: A systematic review. *Renew. Sustain. Energy Rev.* **2016**, *55*, 399–413. [CrossRef]
14. Emmi, G.; Zarrella, A.; Carli, M. De A heat pump coupled with photovoltaic thermal hybrid solar collectors: A case study of a multi-source energy system. *Energy Convers. Manag.* **2017**, *151*, 386–399. [CrossRef]
15. Liu, Z.; Wang, Q.; Wu, D.; Zhang, Y.; Yin, H.; Yu, H.; Jin, G. Operating performance of a solar / air-dual source heat pump system under various refrigerant fl ow rates and distributions. *Appl. Therm. Eng.* **2020**, *178*, 115631. [CrossRef]
16. Italian Interministerial Decree 26th June 2015: Application of Calculation Methods for Energy Performance and Definition of Minimum Building Requirements Italian Interministerial Decree 26th June 2015: Application of Calculation Methods for Energy Performance and Definition of Minimum Building Requirements. *Off. Gazzette Ital. Repub. n°39 15th July 2015* **2015**, 1–8. Available online: https://www.mise.gov.it/images/stories/normativa/DM_requisiti_minimi.pdf (accessed on 13 January 2023).
17. Peel, M.C.; Finlayson, B.L.; McMahon, T.A. Updated world map of the Köppen-Geiger climate classification. *Hydrol. Earth Syst. Sci.* **2007**, *11*, 1633–1644. [CrossRef]
18. *UNI/TS 11300–1*; Building Energy Performance–Part 1: Evaluation of the Energy Need for Space Heating and Cooling. Ente Nazionale Italiano di Unificazione (UNI): Milan, Italy, 2014. (In Italian)
19. CTI-Italian Thermotechincal Committee. Available online: https://www.cti2000.it/ (accessed on 13 July 2021).
20. Bruno, R.; Bevilacqua, P.; Arcuri, N. Assessing cooling energy demands with the EN ISO 52016-1 quasi-steady approach in the Mediterranean area. *J. Build. Eng.* **2019**, *24*, 100740. [CrossRef]
21. Bevilacqua, P.; Perrella, S.; Bruno, R.; Arcuri, N. An accurate thermal model for the PV electric generation prediction: Long-term validation in different climatic conditions. *Renew. Energy* **2021**, *163*, 1092–1112. [CrossRef]
22. *UNI/TS 11300–4*; Building Energy Performance–Part 4: Use of Renewable Energies and Other Generation Methods for Winter Air Conditioning and for the Production of Domestic Hot Water. Ente Nazionale Italiano di Unificazione (UNI): Milan, Italy, 2016. (In Italian)
23. Bevilacqua, P.; Perrella, S.; Cirone, D.; Bruno, R.; Arcuri, N. Efficiency improvement of photovoltaic modules via back surface cooling. *Energies* **2021**, *14*, 895. [CrossRef]
24. Pinamonti, M.; Prada, A.; Baggio, P. Rule-based control strategy to increase photovoltaic self-consumption of a modulating heat pump using water storages and building mass activation. *Energies* **2020**, *13*, 6282. [CrossRef]
25. Bevilacqua, P.; Bruno, R.; Rollo, A.; Ferraro, V. A novel thermal model for PV panels with back surface spray cooling. *Energy* **2022**, *255*, 124401. [CrossRef]
26. Solar Energy Laboratory, University of Wisconsin-Madison. *User Manual: TRNSYS 18 a TRaN Sient SYstem Simulation Program*; TRNSYS Library, Volume 4 Mathematical Reference; Solar Energy Laboratory, University of Wisconsin-Madison: Madison, WI, USA, 2016.
27. Bruno, R.; Nicoletti, F.; Cuconati, G.; Perrella, S.; Cirone, D. Performance indexes of an air-water heat pump versus the capacity ratio: Analysis by means of experimental data. *Energies* **2020**, *13*, 3391. [CrossRef]
28. Diefenbach, N.; Loga, T.; Dascalaki, E.; Balaras, C.; Šijanec Zavrl, M.; Rakušček, A.; Corrado, V.; Corgnati, S.P.; Ballarini, I.; Renders, N.; et al. *Application of Building Typologies for Modelling the Energy Balance of the Residential Building Stock*; Institut Wohnen und Umwelt GmbH: Darmstadt, Germany, 2012; ISBN 9783941140233.
29. Latõšov, E.; Volkova, A.; Siirde, A.; Kurnitski, J.; Thalfeldt, M. Primary energy factor for district heating networks in European Union member states. *Energy Procedia* **2020**, *116*, 69–77. [CrossRef]